

Acoustic Fatigue Research for Honeycomb Sandwich Structure with Impact Damage Based on Vibro-Acoustic Coupling Analysis

Ruowei Li

School of Aeronautics and Astronautics, Shanghai Jiao Tong University, Shanghai, China

TEL:+86 18521947107

E-mail: liruowei@sjtu.edu.cn

Haitao Zhao

School of Aeronautics and Astronautics, Shanghai Jiao Tong University, Shanghai, China

TEL:+86 15000626903

E-mail: zht@sjtu.edu.cn

Mingqing Yuan

School of Aeronautics and Astronautics, Shanghai Jiao Tong University, Shanghai, China

TEL:+86 17321257256

E-mail: yuanmq@sjtu.edu.cn

Ji'an Chen

School of Aeronautics and Astronautics, Shanghai Jiao Tong University, Shanghai, China

TEL:+86 13916958169

E-mail: ja-chen@sjtu.edu.cn

Abstract: Composite honeycomb sandwich structure is widely used in aircraft wing leading edge, rudder surface, engine fairing, etc. It is susceptible to strong aerodynamic noise and impact loads from birds, hails and stones. Therefore, it is essential to evaluate the life of structure with sound and collision load. In this paper, an acoustic fatigue life evaluation method based on vibro-acoustic coupling with impact damage is proposed. A representative composite honeycomb sandwich structure is built up to implement the proposed method. Firstly, the low-velocity impact process is simulated by the finite element (FE) method. This analysis case is used to get the structure with damage and material degradation. Secondly, the FE model is linked with the acoustic indirect boundary element (BE) model. A white Gaussian noise load is applied to the coupled FE/indirect BE model, and the power spectra density (PSD) curve of the structural dangerous point is obtained by modal based vibro-acoustic coupling response case and random post-processing analysis case. At last, the fatigue life of the honeycomb structure is computed by the PSD theory. The result shows that with the increase of the impact energy, the structural life under the same acoustic load decreases. This method reveals high computational efficiency and excellent feasibility. The analytical result has reference value for the acoustic and mechanical properties design of composite honeycomb sandwich structure.

Keywords: *vibro-acoustic coupling; low-velocity impact damage; acoustic fatigue*

1. Introduction

Honeycomb structure ^[1] has advantages as a special composite material, such as light weight, fatigue resistance, high strength, high rigidity and strong heat resistance. So, it has been widely used in aircraft rudder surface, engine fairing, wing tip, floor and interior, etc. The aircraft has been in a strong noise environment during take-off, landing and flight. Long-term high-intensity noise excitation leads to dynamic response and then acoustic fatigue will occur in the structure^[2-3].

During the flight, the aircraft is vulnerable to impact loads such as bird strikes, hail, gravel impact, etc. The honeycomb sandwich panel made of composite material is very sensitive to impact loads and its mechanical performance will change a lot under impact. After the low-velocity impact, it is difficult to see the damage defects only on the surface of the laminate without the aid of the inspection tool. However, complex damages are generated in the interior of the laminate such as fiber breakage, matrix fracture and delamination. These internal damages seriously degrade the structural properties of the laminate and the strength can be reduced by 35%-40%. The reduction in strength will definitely affect the acoustic fatigue life of the structure.

At present, the methods of calculating acoustic fatigue life are mainly divided into two methods: time domain method and frequency domain method. The main method in the time domain is the rain flow counting method^[4-6]. This method requires loop counting and the amount of data processing is very large. Therefore, the current mainstream method is the random vibration fatigue life assessment based on the stress probability density function and the power spectral density method^[7-8] in the frequency domain^[9]. The frequency domain method can overcome this shortcoming. Therefore, random vibration fatigue life assessment method in frequency domain is popular which is based on the stress probability density function and the power spectral density method. In the meanwhile, research on the low-velocity impact of composite materials has gradually matured. Through the simulation by finite element software and the experiment verification, the damage results of the structures with different materials and different layers after low-velocity impact can be obtained. However, no research has been conducted on the acoustic fatigue life of structures subjected to impact loads.

Aiming at this problem, this paper firstly obtains the stiffness degradation of the structure and the deformed model by performing low-velocity impact simulation^[13-14] on the honeycomb sandwich structure. Then, the acoustic-vibration coupling^[10-12] analysis of the honeycomb sandwich panel is conducted under strong noise load. At last, the acoustic fatigue life can be predicted by the power spectral density method.

2. Theoretical considerations

2.1 Hashin criterion & Stiffness degradation criterion

If the influence of the inter layer stress is neglected, the damage of the monolayer is determined by the two-dimensional Hashin criterion, which can be described as followed:

Fiber tensile failure:

$$\left(\frac{\sigma_1}{X_t}\right)^2 + \left(\frac{\tau_{12}}{S_{12}}\right)^2 \geq 1, \quad \sigma_1 \geq 0 \quad (1)$$

Fiber compression failure:

$$\left(\frac{\sigma_1}{X_c}\right)^2 \geq 1, \quad \sigma_1 \leq 0 \quad (2)$$

Matrix tensile or shear failure:

$$\left(\frac{\sigma_2}{Y_t}\right)^2 + \left(\frac{\tau_{12}}{S_{12}}\right)^2 \geq 1, \quad \sigma_2 \geq 0 \quad (3)$$

Matrix compression or shear failure:

$$\left(\frac{\sigma_2}{Y_c}\right)^2 + \left(\frac{\tau_{12}}{S_{12}}\right)^2 \geq 1, \quad \sigma_2 \leq 0 \quad (4)$$

Where, X_t is the longitudinal tensile strength of a monolayer, X_c is the longitudinal compressive strength of a monolayer, S_{12} is the shear strength of the monolayer 1-2 direction.

The material stiffness will be reduced when the failure mode of the above equation is satisfied. According to Reifsnider K.L.^[15], if a point fails, the material stiffness reduction is only limited to the vicinity of this point. The degradation model in this paper uses the Camanho degradation model.

Assuming that a kind of damage can occur in a element, it is necessary to calculate cumulative damage, such as matrix and fiber tensile failure. However, if the matrix or fiber is subjected to tensile failure, the compression failure cannot occur at same elements. If elements have multiple failure modes at the same time, the corresponding degradation parameters are accumulated. The specific methods for material degradation are as follows:

Matrix tensile or shear cracking:

$$E'_2 = 0.2E_2, \quad G'_{12} = 0.22G_{12}, \quad \nu'_{12} = 0.15\nu_{12} \quad (5)$$

Matrix compression or shear cracking:

$$E'_2 = 0.4E_2, \quad G'_{12} = 0.4G_{12}, \quad \nu'_{12} = 0.15\nu_{12} \quad (6)$$

Fiber tensile fracture:

$$E'_1 = 0.07E_1, \quad E'_2 = 0.07E_2, \quad G'_{12} = 0.07G_{12}, \quad \nu'_{12} = 0.07\nu_{12} \quad (7)$$

Fiber compression fracture:

$$E'_1 = 0.14E_1, \quad E'_2 = 0.14E_2, \quad G'_{12} = 0.14G_{12}, \quad \nu'_{12} = 0.14\nu_{12} \quad (8)$$

Matrix stretching or shear cracking and fiber tensile fracture occur:

$$E'_1 = 0.07E_1, \quad E'_2 = 0.2E_2, \quad G'_{12} = 0.22G_{12}, \quad \nu'_{12} = 0.15\nu_{12} \quad (9)$$

Matrix compression or shear cracking and fiber compression cracking occur:

$$E'_1 = 0.14E_1, \quad E'_2 = 0.4E_2, \quad G'_{12} = 0.4G_{12}, \quad \nu'_{12} = 0.15\nu_{12} \quad (10)$$

Where E_i, ν_{ij}, G_{ij} is the current material parameters of the monolayer. E'_i, ν'_{ij}, G'_{ij} is the material parameter of the degradation of the monolayer after failure.

2.2 Metal material constitutive relationship & Failure mode

The plastic properties of the metal material is defined by the Johnson-Cook constitutive:

$$\sigma = [A + B(\bar{\varepsilon}^{pl})^n][1 + C \ln(\dot{\varepsilon}^{pl} / \dot{\varepsilon}_0)] \left[1 - \left(\frac{T - T_r}{T_m - T_r} \right)^m \right] \quad (11)$$

Table 1 Nomenclature & Unit

	Name	Unit
σ	Stress	MPa
A	Initial yield stress at reference temperature	Mpa
B	Strain hardening coefficient at reference temperature	Mpa
C	Strain rate sensitivity index	-
n	Strain hardening index at reference temperature	-
$\bar{\varepsilon}^{pl}$	Plastic strain	-
$\dot{\varepsilon}^{pl}$	Plastic strain rate	-
$\dot{\varepsilon}_0$	Reference strain rate.	-
m	Thermal softening index at reference temperature	-
T	Current temperature	K
T_r	Reference temperature	K
T_m	Melting temperature	K

Damage determination uses maximum failure plastic strain:

$$\varepsilon_f = \left[d_1 + d_2 \exp\left(d_3 \frac{p}{\sigma_e} \right) \right] \left[1 + d_4 \ln\left(\frac{\dot{\varepsilon}}{\dot{\varepsilon}_0} \right) \right] \left(1 + d_5 \frac{T - T_r}{T_m - T_r} \right) \quad (12)$$

Where d_1-d_5 are failure parameters and p is the three-dimensional average stress and σ_e is the Von-Mises equivalent stress.

In the above equations, the first bracket indicates that the strain at break decreases as the hydrostatic tension increases, the second bracket indicates the effect of strain rate, the third bracket indicates the effect of temperature.

2.3 Vibro-acoustic coupling

A coupling coefficient λ_c can be used to determine whether coupling is needed:

$$\lambda_c = \frac{\rho_0 c}{\rho_i T \omega} \quad (13)$$

Where, ρ_0 is the density of the fluid, c is the flow velocity of the sound in the fluid, ρ_i is the density of the structure, T is the equivalent thickness of the structure, ω is the angular frequency.

While $\lambda_c > 1$, vibro-acoustic coupling analysis needs to be done. While $\lambda_c \ll 1$, coupling condition could be neglected.

The coupling equation is:

$$\begin{bmatrix} K_s + j\omega C_s - \omega^2 M & L_c & 0 \\ L_c^T & \frac{D_{11}}{\rho_0 \omega^2} & \frac{D_{12}}{\rho_0 \omega^2} \\ 0 & \frac{D_{21}}{\rho_0 \omega^2} & \frac{D_{22}}{\rho_0 \omega^2} \end{bmatrix} \begin{bmatrix} u_i \\ \mu_{i1} \\ \mu_{i2} \end{bmatrix} = \begin{bmatrix} F_s \\ F_{a1} \\ F_{a2} \end{bmatrix} \quad (14)$$

Where, K_s , C_s , M_s , D_{ij} is the stiffness matrix, damping matrix, mass matrix and coefficient matrix of the structure respectively. u_i is the displacement of each node. μ_{i1} is the sound pressure difference between two sides of the mesh which sound field and structure is coupling, μ_{i2} is the sound pressure difference between two sides of the mesh which sound field and structure is not coupling. F_s is the external force loading on the structure (excluding the sound pressure load). F_{a1} is the sound pressure loading on the sound field-structure coupled mesh, F_{a2} is the sound pressure loading on the uncoupled mesh of the sound field. L_c is the coupling matrix.

2.4 Random acoustic

As for a random process, the PSD matrix \mathbf{S}_{XX} of the input load and the PSD matrix \mathbf{S}_{YY} of the output response can be described by the transfer function matrix \mathbf{H} :

$$\mathbf{S}_{YY} = \mathbf{H}^* \mathbf{S}_{XX} \mathbf{H}^T \quad (15)$$

The input load \mathbf{S}_{XX} can be decomposed while principal component analysis via SVD decomposition or Schur decomposition:

$$\mathbf{S}_{XX} = \tilde{\mathbf{X}}^* \mathbf{S}_{qq} \tilde{\mathbf{X}}^T \quad (16)$$

Where, $\tilde{\mathbf{X}}$ is a matrix determined by each element named principal component. \mathbf{S}_{qq} is a cross-spectral matrix of a random participation factor \mathbf{q} . It can be obtained by equation (15,16).

$$\mathbf{S}_{YY} = \mathbf{H}^* \tilde{\mathbf{X}}^* \mathbf{S}_{qq} \tilde{\mathbf{X}}^T \mathbf{H}^T = \mathbf{Y}^* \mathbf{S}_{qq} \mathbf{Y}^T \quad (17)$$

In general, structural responses can be represented by modal superposition:

$$\tilde{\mathbf{Y}} = \mathbf{\Phi} \mathbf{p} \quad (18)$$

Where, $\mathbf{\Phi}$ is the modal stress vector. \mathbf{p} is the modal random participation factor.

Therefore, it can be written as:

$$\mathbf{S}_{YY} = \mathbf{\Phi}^* \mathbf{p}^* \mathbf{S}_{qq} \mathbf{p}^T \mathbf{\Phi}^T = \mathbf{\Phi}^* \mathbf{S}_{pp} \mathbf{\Phi}^T \quad (19)$$

$$\mathbf{S}_{pp} = \mathbf{p}^* \mathbf{S}_{qq} \mathbf{p}^T \quad (20)$$

2.5 Power spectral density method

The cross-power spectrum curves of each node of the structure are obtained by numerical calculation. The PSD curve of the dangerous point can be obtained by superposition of stationary stochastic processes. And it can be used as an input to calculate the life of acoustic fatigue by power spectral density method.

Acoustic fatigue life can be expressed by equation (21).

$$T = \frac{C}{E(M_T) \int_0^\infty P(s) s^b ds} \quad (21)$$

Where, T is the life of structural acoustic fatigue, b and C are the material constants of S-N curve, $E(M_T)$ is the average incidence of stress cycles per unit time, $P(s)$ is the probability density function of stress, s is stress.

S-N curve can be fitted as a power function:

$$C = Ns^b \quad (22)$$

S-N curve used here has a range of 10^2 - 10^6 cycles.

If the random process is a narrowband random process, $E(M_T)$ is zero crossing rate $E(0)$. If it is a wideband random process, $E(M_T)$ is the peak occurrence rate $E(p)$, as shown in equation (23).

$$E(0) = \sqrt{\frac{m_2}{m_0}}, \quad E(p) = \sqrt{\frac{m_4}{m_2}} \quad (23)$$

m_n is the n th order inertia moment of the stress power spectral density.

$$m_n = \int f^n G(f) df \quad (24)$$

Where, f is the frequency and $G(f)$ is the stress power spectral density function of the dangerous point. The relationship between the acceleration power spectral density function $G_g(f)$ and the stress power spectral density function can be expressed as:

$$G(f) = \frac{H^2}{\omega^4} G_g(f) \quad (25)$$

Where, H is related to the material and structure form and the position of the action reference and the response points. H can be expressed approximately by equation (26).

$$H = \frac{\sigma}{A} \quad (26)$$

Where, σ is the stress at the response point, A is the displacement at the point of action.

In order to determine whether a stationary random process belongs to a wideband process or a narrowband process, an irregular factor is introduced:

$$\gamma = \frac{m_2}{\sqrt{m_0 m_4}} \quad (27)$$

While the irregularity factor is close to 0, the stationary stochastic process can be described as a broadband random process. While the irregular factor is close to 1, it can be described as a narrowband process.

If the random stress process is a narrowband process, the probability density function satisfies Rayleigh distribution which is:

$$P_p(s) = \frac{S}{\sigma_s^2} e^{\frac{-s^2}{2\sigma_s^2}} = \frac{S}{m_0} e^{\frac{-s^2}{2m_0}} \quad (28)$$

The probability density function of a broadband random process is a kind of distribution between Gauss distribution and Rayleigh distribution. It can be described as Dirlik^[8] equation which obtained by Monte Carlo method. It is a semi-empirical equation with good precision.

3. Numerical simulation

3.1 Technical route

The technical route of random vibration acoustic fatigue life assessment used in this paper is shown in Figure 1.

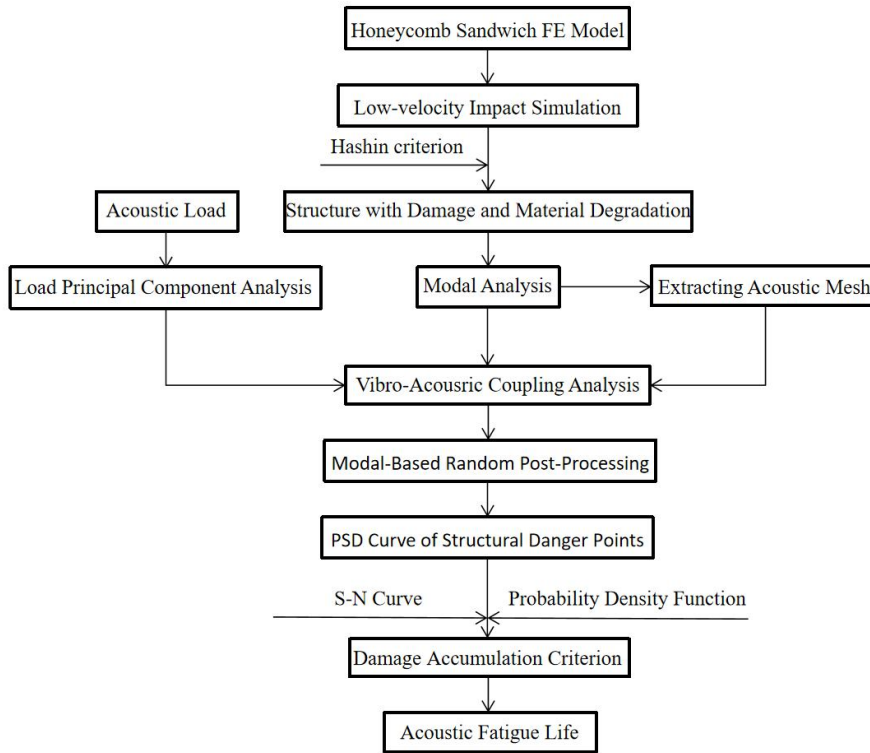


Figure 1 Technical road map

Firstly, the low-velocity impact simulation is carried out by finite element software. The stiffness degradation model of the composite material and the geometric structure after deformation of the material are obtained by Hashin failure criterion. Secondly, the structure should be used the modal analysis and extracted sound field on the surface of the structure in order to get boundary element mesh. Thirdly, the principal component analysis^[16] is applied to the input acoustic load in order to reduce the amount of calculation in the subsequent calculation process. Fourthly, use vibro-acoustic coupling analysis^[17]. Apply modal superposition method for modal-based random sound field post-processing. So that the PSD curve of the dangerous point can be obtained. Fifthly, select the appropriate probability density function by the value of the irregularity factor. Combine S-N curve of the material to get the acoustic fatigue life of the structure.

In this paper, the damaged structures under different impact energy are obtained by different initial velocity. Then the acoustic fatigue life of the structures under the same sound pressure level is calculated.

3.2 Modeling

The overall size of the honeycomb sandwich structure is 300mm×207.846mm×20.6mm. Upper and lower panels are 0.3mm thick. The honeycomb core height is 20mm, regular hexagonal honeycomb structure side length $L=15\text{mm}$, wall thickness $t=0.06\text{mm}$. Punch is modeled by analytical rigid body with a radius of 15mm and a mass of 100g. The geometric model is shown in Figure 2. The detail of the honeycomb structure is shown in Figure 3.

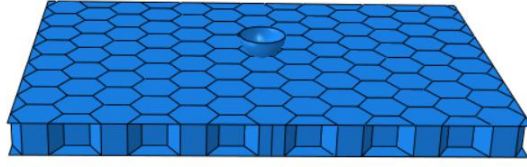


Figure 2 Geometric model

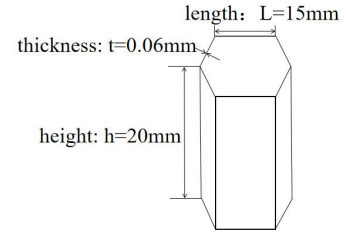


Figure 3 The detail of the honeycomb

While acoustic software Virtual.lab Acoustic is used to simulate, the size of the mesh should be consistent. Encryption of the local mesh can not improve the accuracy because the calculation accuracy of the fluid model is controlled by most elements.

If the highest frequency f_{\max} is known, all elements length L should satisfy:

$$L \leq \frac{c}{6f_{\max}} \quad (29)$$

However, in the structural analysis, the mesh should be refined in places where the stress and displacement gradients are large, or in the vicinity of the sound source, the sharp corners, the holes, etc.

The honeycomb sandwich structure is divided into the upper and lower panels and an intermediate honeycomb core. The upper and lower panels are made of E-Glass/epoxy composite material. The honeycomb cores are all made of LY12CZ aluminum alloy. The composite properties and ply information are shown in Table 2. The properties of LY12CZ are shown in Table 3. The properties of the air material are shown in Table 4. Due to the low-velocity impact, the influence of temperature on the material can be neglected for the Johnson-Cook constitutive used in aluminum alloy materials.

Table 2 E-Glass/epoxy composite material

	Name	Value
	Density: ρ	$1.5 \times 10^3 \text{kg/m}^3$
Ply information	Monolayer thickness	0.125mm
	Lap angle	$[0/90]_s$
	E_{11}	42GPa
Monolayer material properties	E_{22}	11.3GPa
	ν_{12}	0.3
	G_{12}	4.5GPa
	X_T	900MPa
	X_C	900MPa
Monolayer strength parameter	Y_T	50MPa
	Y_C	140MPa
	S_{12}	72MPa
Fatigue parameter:	C	1.87732×10^{10}

b	1.98216
---	---------

Table 3 LY12CZ material

	Name	Value
	Density: ρ	$2.7 \times 10^3 \text{kg/m}^3$
Elastic parameter	Young's modulus: E	70GPa
	Poisson's ratio: ν	0.3
	Initial yield stress at reference temperature: A	324MPa
Plasticity parameter	Strain hardening coefficient: B	114MPa
	Strain rate sensitivity index: C	0.0026
	Strain hardening index: n	0.42
	Quasi-static reference strain rate $\dot{\epsilon}_0$	1
Plastic failure parameter	No.1 fracture parameter: d_1	-0.77
	No.2 fracture parameter: d_2	1.45
	No.3 fracture parameter: d_3	0.47
	No.4 fracture parameter: d_4	0
	No.5 fracture parameter: d_5	0
Fatigue parameter	Fatigue parameter: C	3.0218×10^{19}
	Fatigue parameter: b	6.447

Table 4 Air material

Name	Value
Sound velocity: c	340m/s
Density: ρ	1.225kg/m^3

The load is 163 dB Gaussian white noise applied on the band range of 10-2500 Hz which step size is 10 Hz. The PSD curve can be obtained by the equation (30) and applied as a load on the acoustic mesh surface of the entire model. The acoustic mesh is a two-dimensional boundary element mesh extracted from the surface of the structure. The honeycomb sandwich structure is modeled by the shell element, so the mesh of the acoustic and the structure is consistent. Reference sound pressure $p_0 = 2 \times 10^{-5}$ Pa.

$$\text{dB} = 10 \times \log_{10} \left(\frac{P}{P_0} \right)^2 \quad (30)$$

4. Results and discussion

4.1 Impact simulated results

With low-velocity impact of different velocities, the stress & deformation cloud diagram is shown in Figure4. In order to display the stress level and deformation of the impact point well, the resulting cloud image only shows 1/4 of the structure.

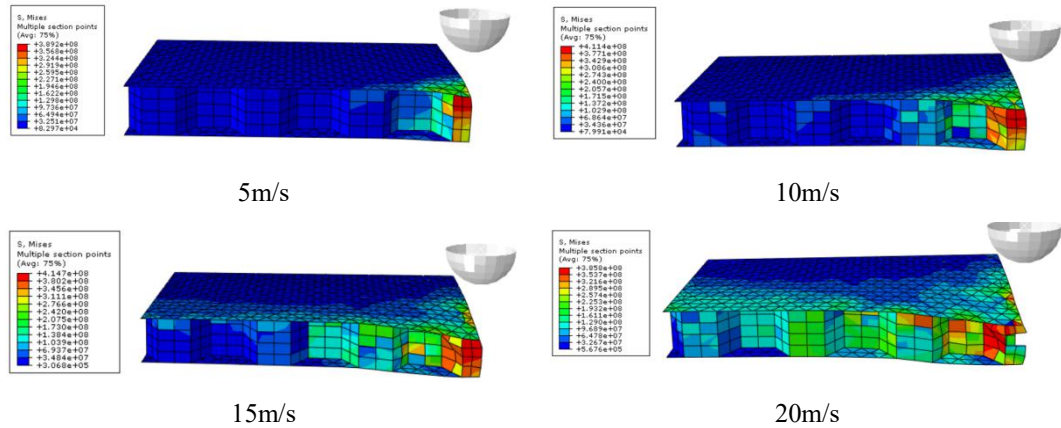


Figure 4 Stress cloud diagram of structures at different impact velocities

It can be clearly seen that as the impact energy increases, the deformation becomes more and more serious. Honeycomb sandwich made of aluminum alloy has been damaged at an impact velocity of 20 m/s.

The damage of the panel is determined by Hashin criterion which can be divided into 6 damage modes are shown in Section 2.1. Figure 6 shows the damage cloud of each layer panel when the impact velocity is 20m/s. The red area indicates that the structure is damaged, the blue color indicates that the structure has not received damage. The ply of panel is named as shown in Figure 5.

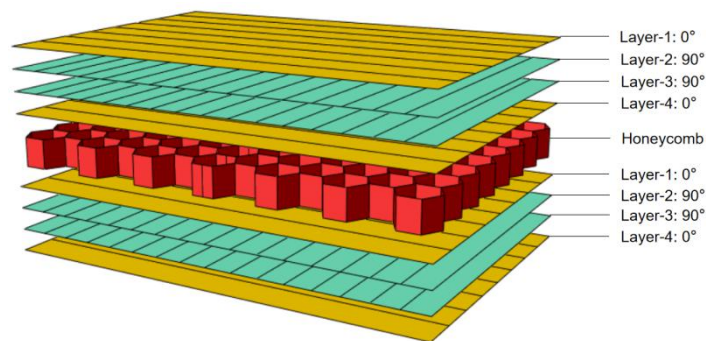
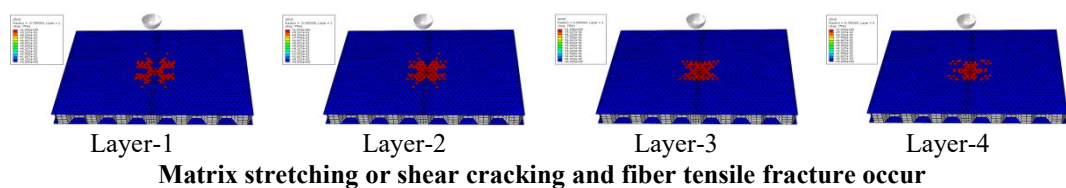


Figure 5 Lamination naming rules



Matrix stretching or shear cracking and fiber tensile fracture occur

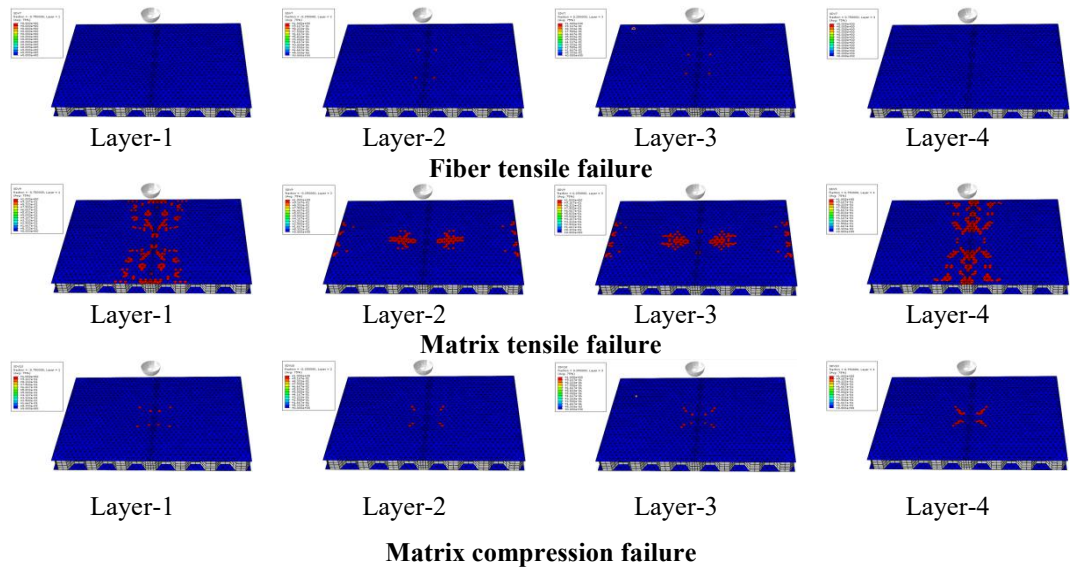


Figure 6 Damage cloud map of each layer under different damage modes

With an impact velocity of 20 m/s, there are only four failure modes in the honeycomb sandwich structure: simultaneous tensile failure of the matrix and fibers, fiber tensile failure, matrix tensile failure and the matrix compression failure. In the area affected by the impact, the main performance is the simultaneous failure of the fiber and matrix, the cross-shaped area centered on the impact point, the main failure mode is the matrix tensile failure, the direction of the failure is perpendicular to the fiber layup direction.

4.2 Acoustic simulation results

4.2.1 Modal analysis

Boundary conditions used in the modal analysis are four-sided clamped. The modal and natural frequencies are inherent properties of the structure. Each natural frequency corresponds to a modality. While the frequency of the external excitation load is close to the natural frequency of a certain order of the structure, the result will produce a corresponding deformation. Since the structure only has different impact energies, the low-order modes of each model have similarities. Only the first three-order modes with an impact velocity of 20m/s and the natural frequencies are given.

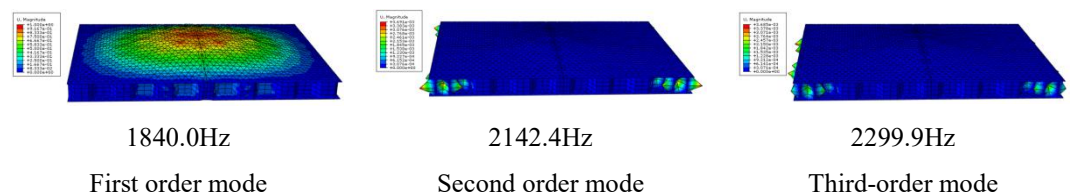


Figure 7 First third mode

4.2.2 Principal component analysis

Principal component analysis is performed on the PSD matrix of the input load by using Schur decomposition with a truncation error of 0.0001. The input power spectral density load can

be extracted as the 53 order principal component. Figure 8 is the main component number increasing with frequency.

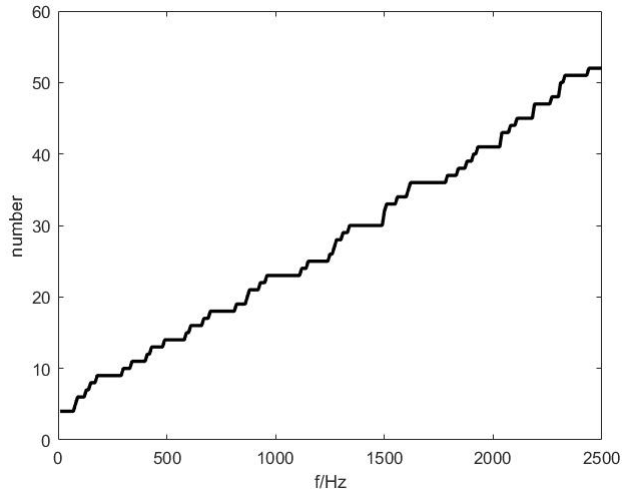


Figure 8 Number of principal components - frequency map

Since the influence of the first few principal components is great, only the auto powerspectrum curve of the first five principal components is shown in Figure 9.

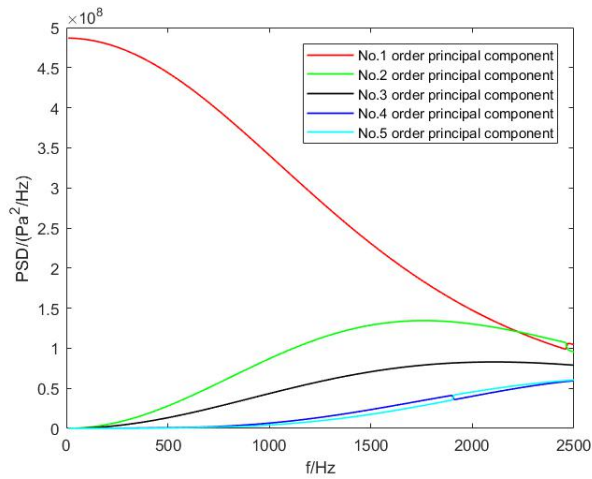


Figure 9 Auto power spectral density curve of the first five orders of principal components

As can be seen from Figure 9, the first-order principal component has a very significant contribution at low and intermediate frequency and is slightly low at high frequency. The remaining main components are lower in the low frequency and have a larger contribution in the middle frequency band.

4.2.3 Acoustic vibration coupling analysis

According to the modal-based acoustic-vibration coupling analysis, the response of the structure at each frequency can be obtained. Figure 10 shows the impact velocity of 20m/s, the displacement cloud map of the first three natural frequency under the first-order principal component. The cloud image shows only 1/4 of the structure.

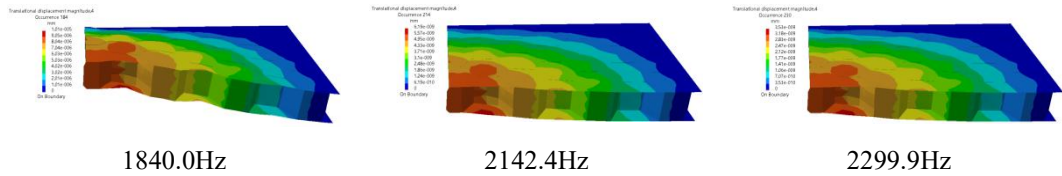


Figure 10 Displacement cloud map of the first three natural frequencies under the first-order principal component

Since the structure is fixed on four sides and is impacted at the center, the portion with a large displacement is located at the center of the plate. The displacement gradually decreases toward the edge of the plate. The low-order mode contributes a lot to the displacement. It can be easily seen that the displacement of the first-order natural frequency is about 100 times larger than the second-order or third-order.

4.2.4 PSD curve

The PSD curve of the dangerous point with the impact velocity of 20m/s is obtained by numerical analysis. Due to the different materials, the PSD curves of the dangerous points of the panel and the honeycomb are respectively shown in Figure 11, 12.

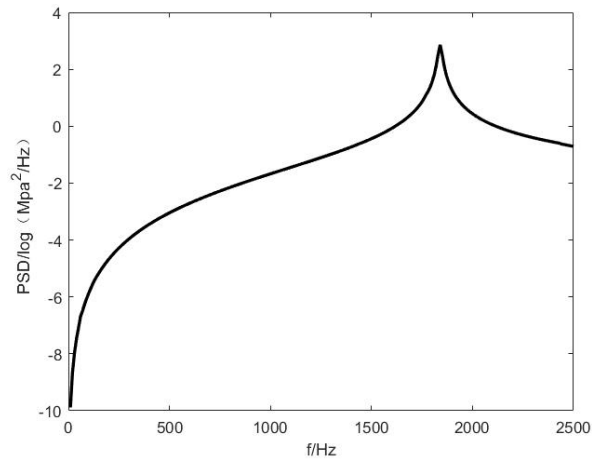


Figure 11 PSD curve of dangerous point on the panel

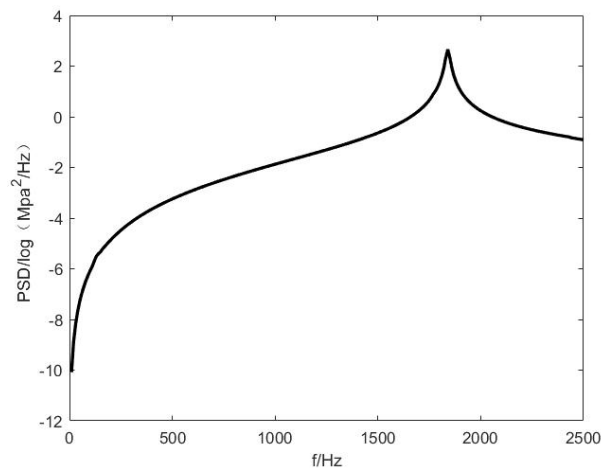


Figure 12 PSD curve of dangerous point on the honeycomb

The PSD curve of the panel and the honeycomb has the same trend. The PSD curve peak value of the panel dangerous point is $721.44\text{Pa}^2/\text{Hz}$, while the honeycomb is $455.59\text{Pa}^2/\text{Hz}$. The peak appears at the first-order natural frequency. The PSD curve shows small jitters in the natural frequencies of the remaining steps. It can be seen that the first-order natural frequency of the structure play an important role in the acoustic lifetime.

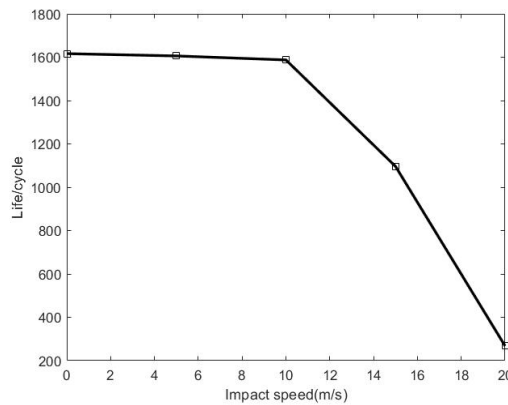
4.3 Acoustic fatigue life

4.3.1 Acoustic fatigue life

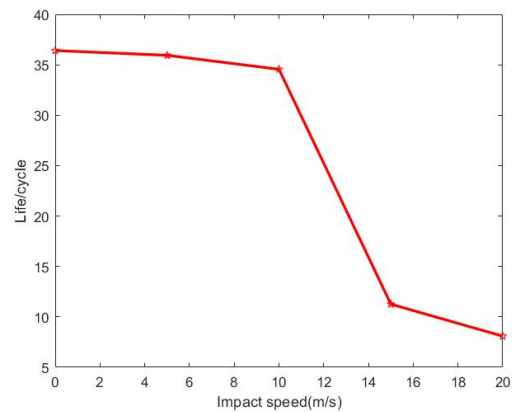
Table 5 and Figure 13 show the structural acoustic fatigue life at different impact velocities under 163dB white noise loading.

Table 5 Lifetime at different velocities

Impact velocity(m/s)	Impact energy(J)	Panel life(cycle)	Honeycomb life(cycle)
0	0	1616.451	36.410
5	1.25	1605.813	35.940
10	5	1587.377	34.552
15	11.25	1096.320	11.266
20	20	267.552	8.087



Panel life



Honeycomb life

Figure 13 Lifetime

Because the panel is made by composite material and the thickness is greater than the wall thickness of the honeycomb, the life of the dangerous point on the panel is much longer than the honeycomb. But the trend of the panel and the honeycomb is the same. While the impact velocity is low, the influence on the acoustic fatigue life is very small. But when the impact velocity exceeds 10 m/s, the acoustic fatigue life of the structure falls off. It can be seen that impact damage has a very serious effect on the life of the structure.

4.3.2 Acoustic fatigue life of structures under different noise loads

In order to determine if the conclusions above are applicable under different load conditions, the structural fatigue life at different loads of 154 dB-163 dB with increments of 3 dB is given below. Table 6, 7 and Figure 14 show the acoustic fatigue life of the structure under different sound loads and different impact velocities. The units not marked in the table are cycles

Table 6 Lifetime of panel under different velocities and different sound loads

Panel	0m/s	5m/s	10m/s	15m/s	20m/s
157dB	160123.579	160087.364	158421.148	123213.215	28915.124
160dB	17220.584	16989.294	16624.487	11842.218	3000.235
163dB	1616.451	1605.813	1587.377	1096.320	267.552

Table 7 Lifetime of honeycomb under different velocities and different sound loads

Honeycomb	0m/s	5m/s	10m/s	15m/s	20m/s
157dB	3710.125	3615.025	3582.215	1200.541	799.254
160dB	371.021	355.992	350.225	108.589	82.104
163dB	36.410	35.940	34.552	11.266	8.087

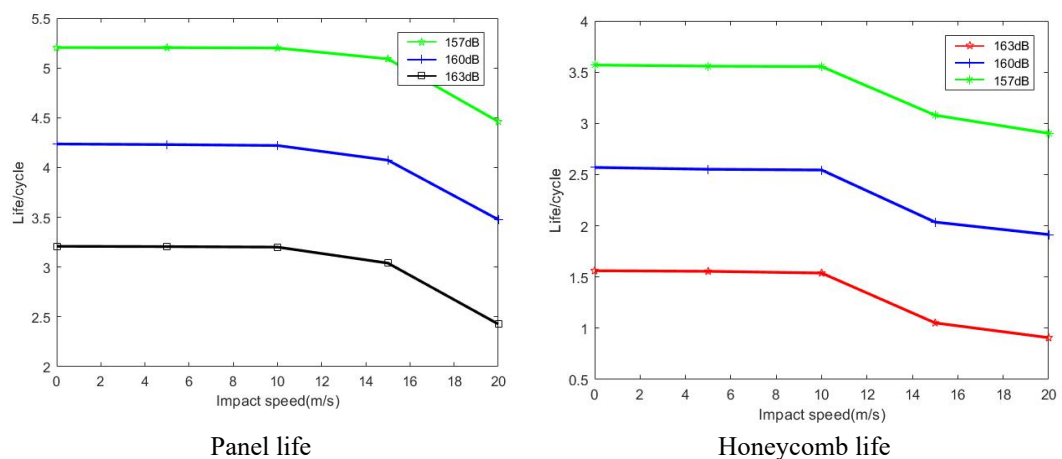


Figure 14 Life table in logarithmic coordinate system

It can be seen from Figure 14 that the life curves of structures under different acoustic loads have similarities. The structural life decreases by an order of magnitude with every 3 dB increment of noise load at the same impact velocity.

5. Conclusions & Outlook

(1) The acoustic fatigue life of the honeycomb sandwich structure is insensitive to low energy impacts. While the impact energy exceeds 5J, the life span decreases greatly.

(2) With every 3 dB increment of acoustic load, the life of the honeycomb sandwich structure is reduced by an order of magnitude.

(3) Using the power spectral density method to calculate the structural acoustic fatigue life, only need to obtain the response power spectral density curve of the structure and give the corresponding probability density function of the broadband and narrowband, then calculate the acoustic fatigue life of various forms of random processes. It is easily to be complied.

In the future research, the acoustic fatigue life assessment method can be verified and improved by combining the acoustic fatigue experiment. The relationship between honeycomb sandwich structure and acoustic fatigue life of different sizes and different layers can be discussed.

References

- [1] LIU Minjing, WU Zhanjun. Application of composite honeycomb sandwich structure in aircraft[J]. Science & Technology Review, 2016, 34(8):21-25
- [2] White R G. Developments in the acoustic fatigue design process for composite aircraft structures[J]. Composite Structures, 1990, 16(1):171-192. DOI:10.1016/0263-8223(90)90071-L
- [3] Vaicaitis R . Acoustic fatigue - A Monte Carlo approach[M]. AIAA/ASME/ASCE/AHS 28th SDM Conf., Paper 87-0916l, Monterey, CA, April 1987. DOI:10.2514/6.1987-916
- [4] Zhao X, Jiang D, Zhang Q. Application of Rain-flow Counting Method in the Analysis of Load Spectrum[J]. Science & Technology Review, 2009, 27(3):67-73. DOI:10.1109/CLEOE-EQEC.2009.5194697
- [5] Hong N. A modified rainflow counting method[J]. International Journal of Fatigue, 1991, 13(6):465-469. DOI:10.1016/0142-1123(91)90481-d
- [6] JIN Yishan, LI Lin. Sonic Fatigue Life Prediction of Aeroengine Structure[J]. Journal of Aerospace Power, 2003, 18(3):373-377. DOI:10.3969/j.issn.1000-8055.2003.03.013
- [7] XU Fei, XIAO Shouting. The power spectral density method for the estimation of the sonic fatigue life[J]. Journal of Mechanical Strength, 1996(4):38-42.
- [8] WANG Mingzhu. Research on life analysis method for structure vibration fatigue[D]. Nanjing University of Aeronautics and Astronautics, 2009. DOI:10.7666/d.d076113
- [9] Tovo R. Cycle distribution and fatigue damage under broad-band random loading[J]. International Journal of Fatigue, 2002, 24(11):1137-1147. DOI:10.1016/s0142-1123(02)00032-4
- [10] BAI Changqing, ZHOU Jinxiong, YAN Guirong. Effects of Sound Field on Thin-wall Cylindrical Structure Dynamic Characteristics[J]. Journal of Mechanical Engineering. DOI:10.3901/JME.2011.05.078

- [11] Cheng L . Fluid-Structural Coupling Of A Plate-Ended Cylindrical Shell: Vibration And Internal Sound Field[J]. Journal of Sound and Vibration, 1994, 174(5):641-654. DOI:10.1006/jsvi.1994.1299
- [12] Craggs A. Coupling of finite element acoustic absorption models[J]. Journal of Sound & Vibration, 1979, 66(4):605-613.
- [13] Abrate S . Impact on Composite Structures || Low-Velocity Impact Damage[J]. 1998, 10.1017/CBO9780511574504(4):135-160. DOI:10.1017/CBO9780511574504.005
- [14] Fangyu C, Li Z, Yihao T. Damage and residual compressive strength of multi-layer composite laminates after low velocity impact[J]. International Journal of Crashworthiness, 2019:1-7.DOI:10.1080/13588265.2018.1478925
- [15] Reifsnider K L . Fatigue of composite material[J]. Composite Materials Series, 1991, 4(1775):11-77. DOI:10.1007/978-3-7091-2544-1_6
- [16] Tipping M E , Bishop C M . Probabilistic Principal Component Analysis[J]. Journal of the Royal Statistical Society: Series B (Statistical Methodology), 1999, 61(3): 611-622. DOI:10.1134/S10637 71017030071.
- [17] LI Zenggang, ZHAN Fuliang.Virtual.Lab Acoustics Acoustics Simulation Calculation Advanced Application Example[M]. National Defense Industry Press,2010